02

Study of the microstructure of phosphors for laser lighting devices

© S.M. Zuev, A.V. Kretushev

MIREA — Russian Technological University, Moscow, Russia

e-mail: sergei_zuev@mail.ru

Received February 12, 2023 Revised March 14, 2023 Accepted March 14, 2023

A brief description is given of phosphors from various manufacturers that can be used in lighting devices with laser injection in the range of 400−480 nm. An estimate of their energy output and inertia is given. The necessity of studying various types of luminescence to optimize the characteristics of phosphor lighting devices is described. It is known that the optical characteristics of laser lighting devices depend on the quality of the phosphor. However, at the moment there are no well-established methods for studying phosphors for compliance with the requirements for brightness, luminous flux, and thermal degradation. One of these methods can be microscopy, which allows you to study the microstructure of samples. The paper considers a method for determining the geometric and optical parameters of individual phosphor particles used for laser lighting devices using microscopy. On the example of a fine suspension of phosphors, images were obtained and some optical parameters of individual particles with diameters from 40 to 150 nm were determined. The conducted studies demonstrate the high resolution of the microscopy method, which can be used to visualize phosphor particles.

Keywords:phosphor, energy efficiency, microscopy, lighting device, optoelectronic devices and systems.

DOI: 10.61011/EOS.2023.03.56185.4616-22

Lighting technology is currently experiencing a boom in technology, circuit design, construction and new ideas in the field. Finally, more than a century after the invention of the incandescent light bulb, there was a breakthrough in this area as well, with discharge light sources, then luminescent, LED and finally laser luminaires. In all of these types of light sources, phosphors play an important role and can be used to achieve some of the most incredible lighting designs. In this regard, the purpose of this paper is to investigate and describe the physical and chemical characteristics of phosphor systems that can be used in modern illumination devices, as well as their production processes [1].

As we know, phosphors are substances capable of emitting light under the influence of various excitations. These substances may be in a gaseous, liquid or solid state. Solid luminescent substances make up the largest group of substances used to produce luminescent radiation. The main characteristics of phosphors are: energy and quantum yield, excitation and emission spectra, inertia, stability, vacuum properties and cost. The ratio of the luminescence energy to the absorbed excitation energy is called the energy yield [2]. In view of the unavoidable losses, the energy yield is always less than unity. The ratio of the number of quanta of luminescence to the number of absorbed quanta excited by radiation is called the quantum yield. This value can be less than 1, equal to or greater than 1.

The excitation spectrum is determined by the range of wavelengths absorbed by the phosphor and causing its cross section, and the - emission spectrum — the range of wavelengths emitted by the phosphor. The spectral composition of the radiation determines the luminescence color of the phosphor [3].

The inertia of a phosphor refers to the time during which it acquires its normal brightness after excitation has begun or during which the phosphor ceases to glow after its excitation has ceased. The stability of a phosphor is expressed in the retention of its basic luminous properties at a predetermined level for a certain period of time [4].

Activators in many phosphors are the essential component that determines the luminescence of the substance, its chromaticity, etc. Copper, silver, manganese, antimony, titanium etc. are used as activating agents. Sometimes more than one activator is used, but rather two or three. The place where it is introduced into the crystalline lattice of the base substance is the center of the luminescent emission [5]. The activator is administered in the thousandths and ten thousandths of a gram for each gram of base substance. It shall be evenly distributed over the entire mass of the base and be in a bonded state. Excess activator impairs the stability and other important properties of the phosphor [6].

The introduction of two or more activators has two main aims: to obtain radiation from activators in different wavelength ranges and to achieve excitation of the active center if it cannot be directly excited in the usual way [7]. In this case, the activator specifically introduced for excitation is called a sensitizer. An example is calcium halophosphate activated by antimony and manganese. The sensitizer here is antimony [9]. By absorbing ultraviolet radiation from the field of incident radiation, antimony converts part of this energy into its own emission band, and passes the other part to manganese, which, being thus excited, emits a different band [10] from antimony.

Special treatment of phosphor powders can, for example, create thin compound layers on the surface of the phosphor grains, increasing aggregation resistance, stability in the process, changing the electrical properties of the material, etc. This treatment is carried out in vapors or chemical

Table 1. Types of luminescence by type of excitation and by type of luminescence

Name	Type of energy absorption	Type of luminescence
Photoluminescence	Electromagnetic radiation (UV and visible light)	Fast-attenuating
X-ray luminescence	Electromagnetic radiation (X-rays)	Prolonged
Cathodoluminscescence	Kinetic energy of electrons	Fast-attenuating
Electroluminescence	Electric field energy	Fast-attenuating
Chemiluminescence	Chemical reaction energy	Prolonged
Bioluminescence	Biochemical reaction energy	Prolonged
Triboluminescence	Mechanical friction energy	Fast-attenuating
Thermoluminescence	Temperature Energy	Prolonged

Table 2. Main characteristics of phosphor LSID-560 (according to manufacturer)

Indicator name	Norm	Values
Appearance	Fine powder light yellow *	Fine powder light yellow * .
Characteristic odour	Absent	Absent
Wavelength of maximum luminescence spectrum in the visible spectral area, nm, at $\lambda_{max,ex} = 450$ nm	550 ± 10	552 .
Wavelength of the main maximum luminescence excitation in the visible spectral area, nm	450 ± 10	450 .
Brightness in relation to the reference sample, %, min	90	98
Average particle size, μ m	Optional	6,2
Temperature resistance, °C, min	250	350
pH of the aqueous suspension	6.0−8.0	7.0

*Weak shade allowed .

Table 3. Main characteristics of phosphor FLS-540

Indicator name	Analytical results
Brightness in relation to the reference sample, %, min	100
Average particle size, μm	25.6
Presence of foreign matter visible to the naked eye	None

solutions. A large number of luminescence species are currently known, as shown in Table 1.

Because there are so many types of luminescence, the number of modern phosphors is in the hundreds, and the number of substances for making them is in the thousands. But not all of them are suitable for laser illuminators with ultraviolet or blue laser injection. As an example of phosphors which can be used in laser illuminators of this type, Tables 2 and 3 show the main characteristics of Russian produced LSID-560 and FLS-540 phosphors, which have shown good performance when applied in laser illumination systems with blue laser diode injection ($\lambda = 400-480$ nm)

The characteristics of the FLS-540 phosphor used in the laser illuminator are shown in Table 3.

The appearance of LSID-560 and FLS-540 phosphor powders is shown in Fig. 1. Both phosphors — are photoluminescent phosphors that convert UV laser radiation

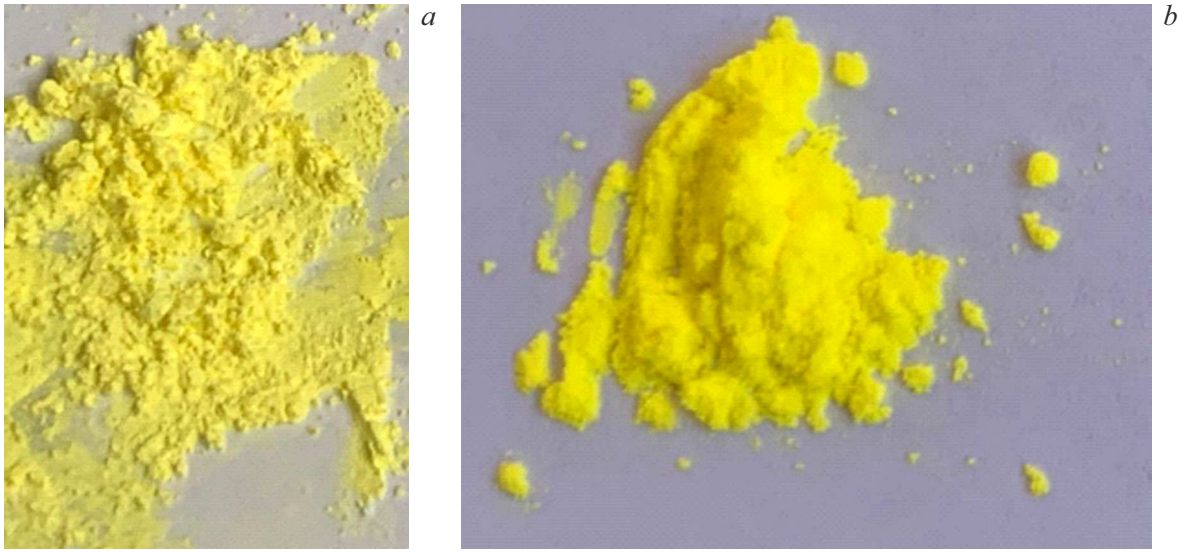

Figure 1. Appearance of LSID-560 (*a*) and FLS-540 (*b*) phosphor powders, obtained by irradiation with an LED with a maximum at 480 nm.

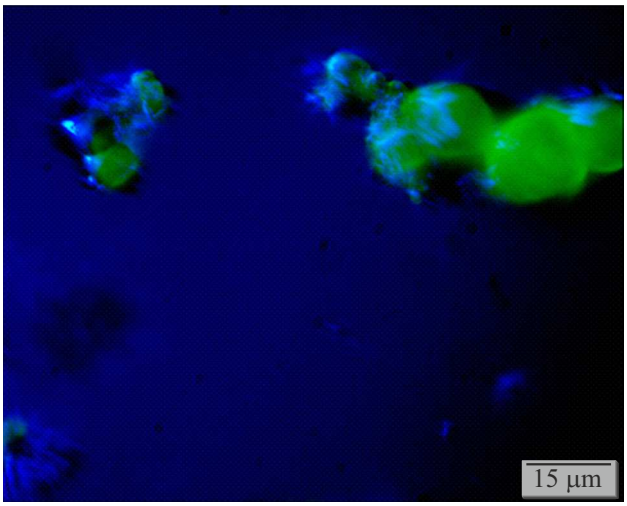

Figure 2.

into -visible light. Such photoluminescence is a mixture of: a base (chlorides, sulphates, borates, fluorides or phosphates of alkali earth metals), a metal-activator, a melt (flux).

The basis of the LSID-560 and FLS-540 phosphors is yttrium aluminum garnet doped with cerium (YAG:Ce $^{3+}$). Let's take a closer look at the characteristics of this compound.

System $Y_3Al_5O_12:Ce^{3+}$ is known as a high performance phosphor for light sources. Its distinctive feature is that it has a well-placed photoluminescence excitation area with maximum at a wavelength of 460 nm. This coincides with the emission maximum of indium-gallium-nitrogen-based chips and is close to that of a laser UV diode with an emission wavelength in range 400−480 nm.

Consider measurements of LSID-560 and FLS-540 phosphor microcrystals using a light microscope. The phosphors were measured with a light microscope. The phosphors were illuminated using a blue LED with a maximum of 480 nm and a white LED. The field size in images with the LOMO 90x NA1.25 lens was $88\times110\,\mu$m.

Let's first look at FLS-540 microcrystals. The initial image of FLS-540 phosphor microcrystals when illuminated by a blue LED with maximum at a wavelength of 480 nm is shown in Fig. 2. Separation by color channel allows the distribution of luminescence intensity in individual phosphor crystals to be observed without a cut-off filter. Under experimental conditions, the blue channel contained glare and background illumination of excitation radiation. There was no luminescence emission intensity in the red channel. The distribution of luminescence intensity in the green channel is shown in Fig. 3 in gradations of grey.

The profile in Fig. 3,*c* shows the boundaries of a microcrystal with a transverse dimension of $8\,\mu$ m. Another distribution of luminescence intensity in the green channel is shown in Fig. 4.

The profile of luminescence intensity distribution in Fig. 4,*c* shows microcrystal boundaries with transverse size $8\,\mu$m.

With additional illumination by a white LED, the image shown in Fig. 5 was obtained, in which the phosphor emission was observed to be transformed over a wider wavelength range. Crystal luminescence was observed not only in the green channel, but also in the red channel of the color image. The intensity distributions in the color channels of the original image and the result of cleaning from the luminescence-exciting light are shown in Figs. 6 and 7.

Images of LSID-560 phosphor microcrystals were obtained under similar conditions. No luminescence was

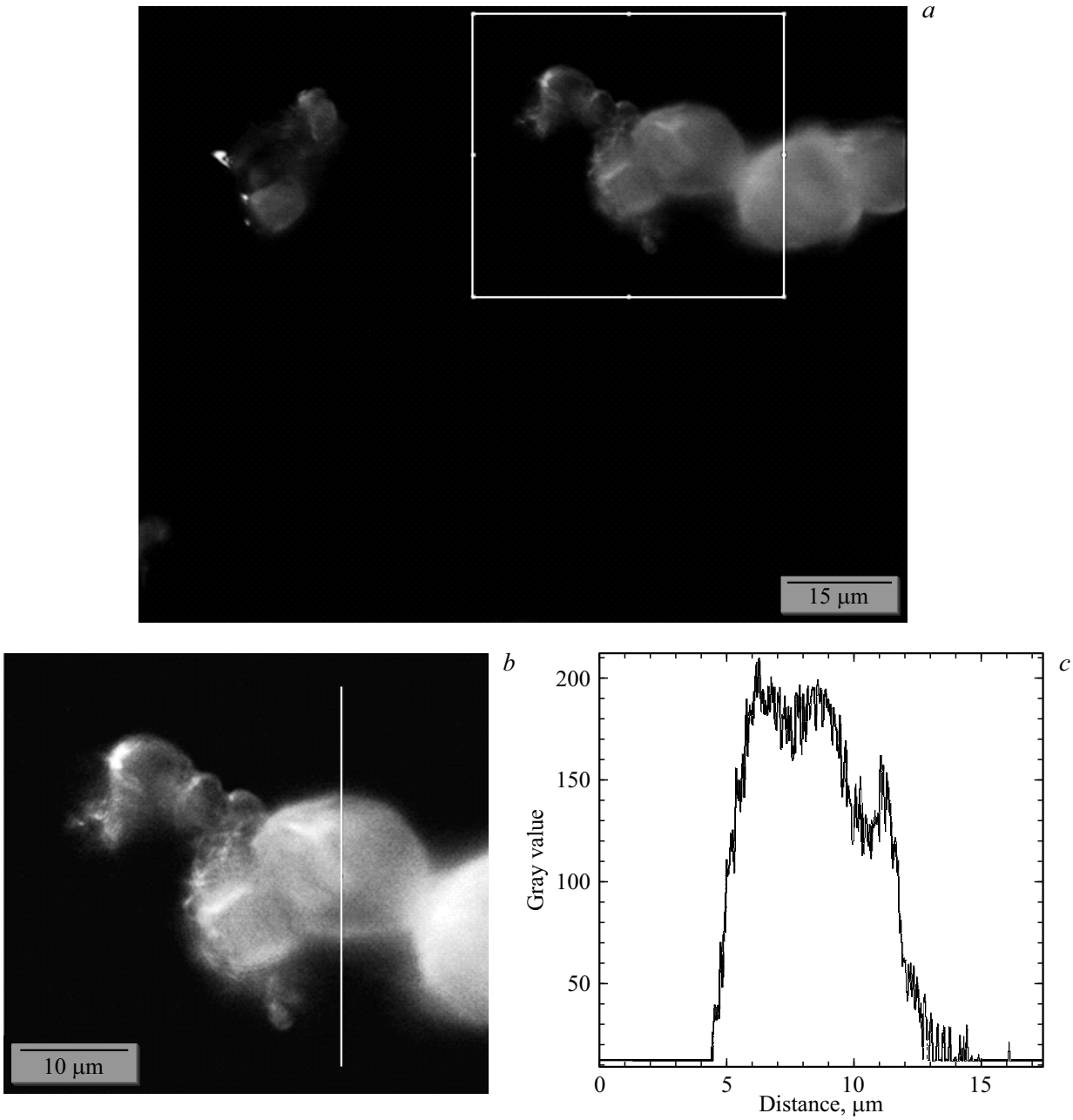

Figure 3. (*a*) Luminescence intensity distribution of FLS-540 phosphor in the green channel (shown in grayscale). (*b*) The image of the selected area in the figure *a*. (*c*) Luminescence intensity distribution profile (in conditional units) along the cross section of the microcrystal (shown by the line in the image on the left).

observed in the image when illuminated only by the blue LED due to the lower emission conversion factor of this phosphor. With some orientation of the sidelight, it was possible to distinguish microcrystals in the image by glare and light absorption. The image (Fig. 7) shows that microcrystals with smaller size ($\sim$2–4 times) prevail than in FLS-540. In addition, the surface of these crystals is considerably less smooth compared to FLS-540.

When using LSID-560 blue and white LEDs in the backlighting of microcrystals, an image was obtained (Fig.8), in which the conversion of the phosphor radiation in the wide range was observed, but in comparison with FLS-540 with a significantly lower conversion coefficient. The intensity distribution was observed in both the green and red channels of the color image. The result of purification from luminescence-exciting radiation in LSID-560 is shown in Fig. 8.

Consider a system of phosphor – glass substrate, with the phosphorreceiving laser radiation with $\lambda = 405$ nm. The phosphor film, as shown in Fig. 1–8, is a set of spherical particles with different diameters d_1, $d_2, \ldots, d_n$. In the general case, the area of the phosphor film will be described

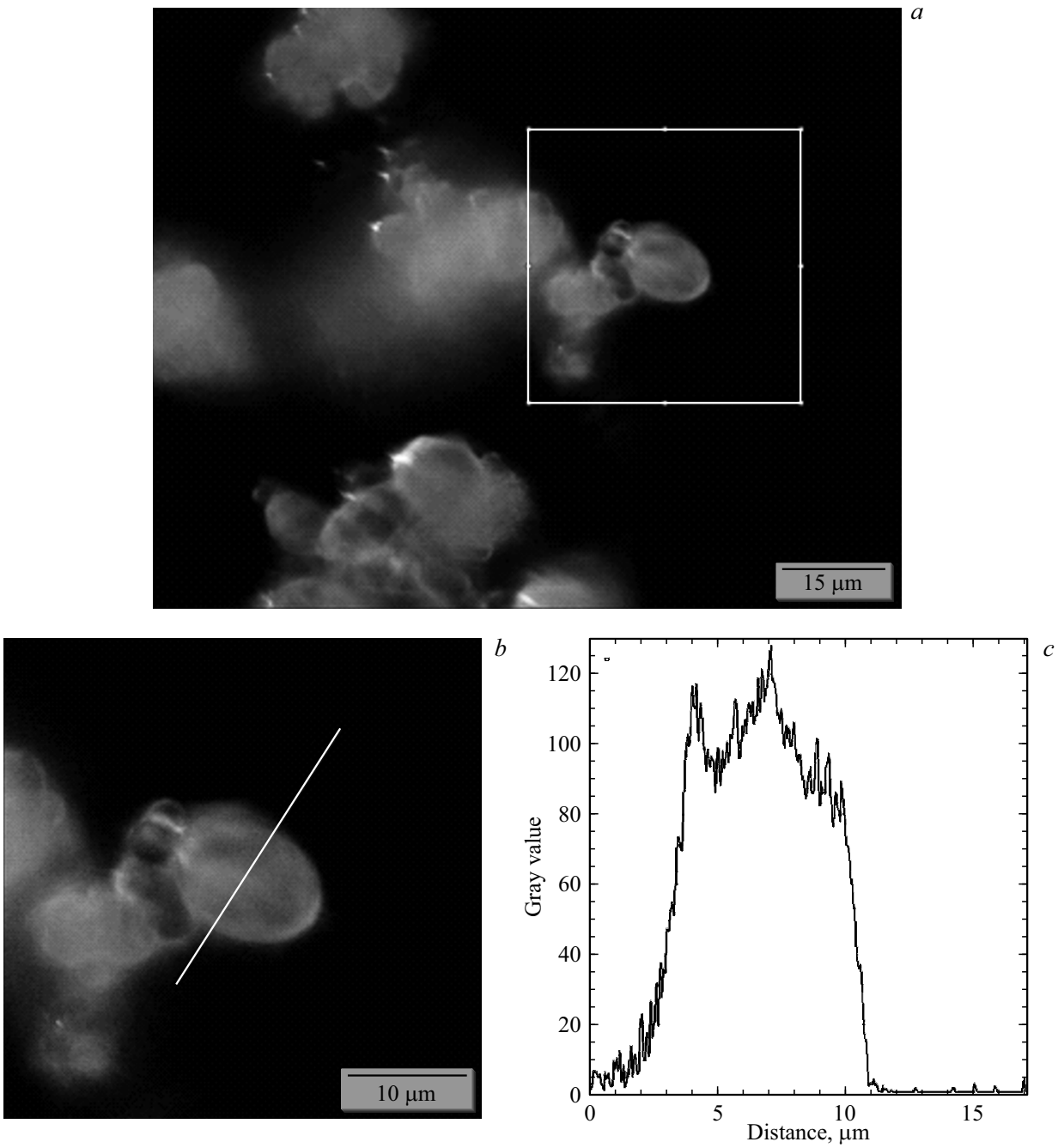

Figure 4. (*a*) Luminescence intensity distribution (in channel green) of the phosphor FLS-540. (*b*) The image of the selected area in the figure *a*. (*c*) Luminescence intensity distribution along the cross section of the microcrystal (shown by the line in the image on the left).

by the formula

$$S = S_{\text{lum}} + S', \tag{1}$$

where S_{lum} — area of phosphor particles, m^2; S' — pore area between phosphor particles, m^2.

The total area of the phosphor particles can be described by an equation of the form

$$S_{\text{lum}} = \frac{1}{N}\left(\frac{\pi d_1^2}{4} + \frac{\pi d_1^2}{4} + \ldots + \frac{\pi d_N^2}{4}\right) = \frac{\pi}{4N}\sum_{i=1}^{N} d_i^2. \tag{2}$$

According to Moivre's theorem, the distribution of the phosphor particles tends to normal, i.e.

$$d(N) = \frac{1}{\sqrt{2\pi\sigma}} \exp\left(\frac{-(N-a)^2}{2\sigma^2}\right). \tag{3}$$

Then,

$$S_{\text{lum}} = \frac{\pi}{4}\left(\frac{a d_{\max}^2}{2}\right), \tag{4}$$

where a — distribution density. Knowing the size of the particles, we can further determine the luminous flux

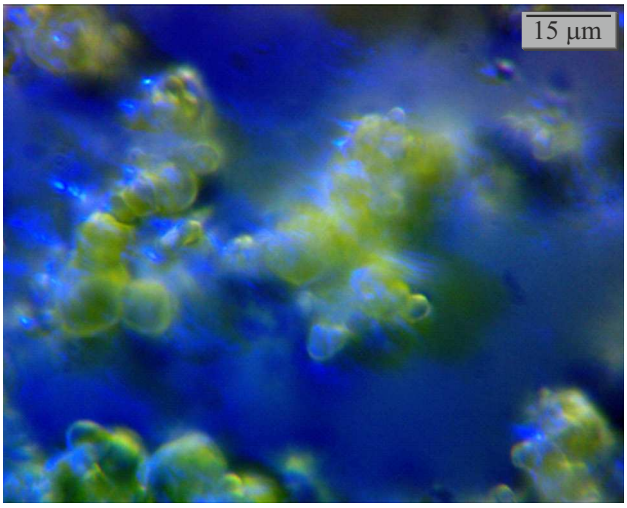

Figure 5. Initial image of phosphor microcrystals when illuminated by blue and white LEDs.

and other optical characteristics of the phosphor, which is beyond the scope of this study.

Conclusions

Analysis of the results of microscopy of LSID-560 and FLS-540 phosphors showed the following.

1. No luminescence of LSID-560 phosphor microcrystals was observed in the red and blue image channels.

2. When using LSID-560 blue and white LEDs in the illumination of microcrystals, an image was obtained (Fig. 7), in which radiation conversion by the phosphor in a wide range was observed, but in comparison with FLS-540 with a significantly lower conversion coefficient.

3. The obtained images of LSID-560 phosphor microcrystals allow us to conclude about a lower conversion coefficient of radiation by this phosphor in comparison with the phosphor FLS-540 due to the absence of luminescence when illuminated only by blue LED. In LSID-

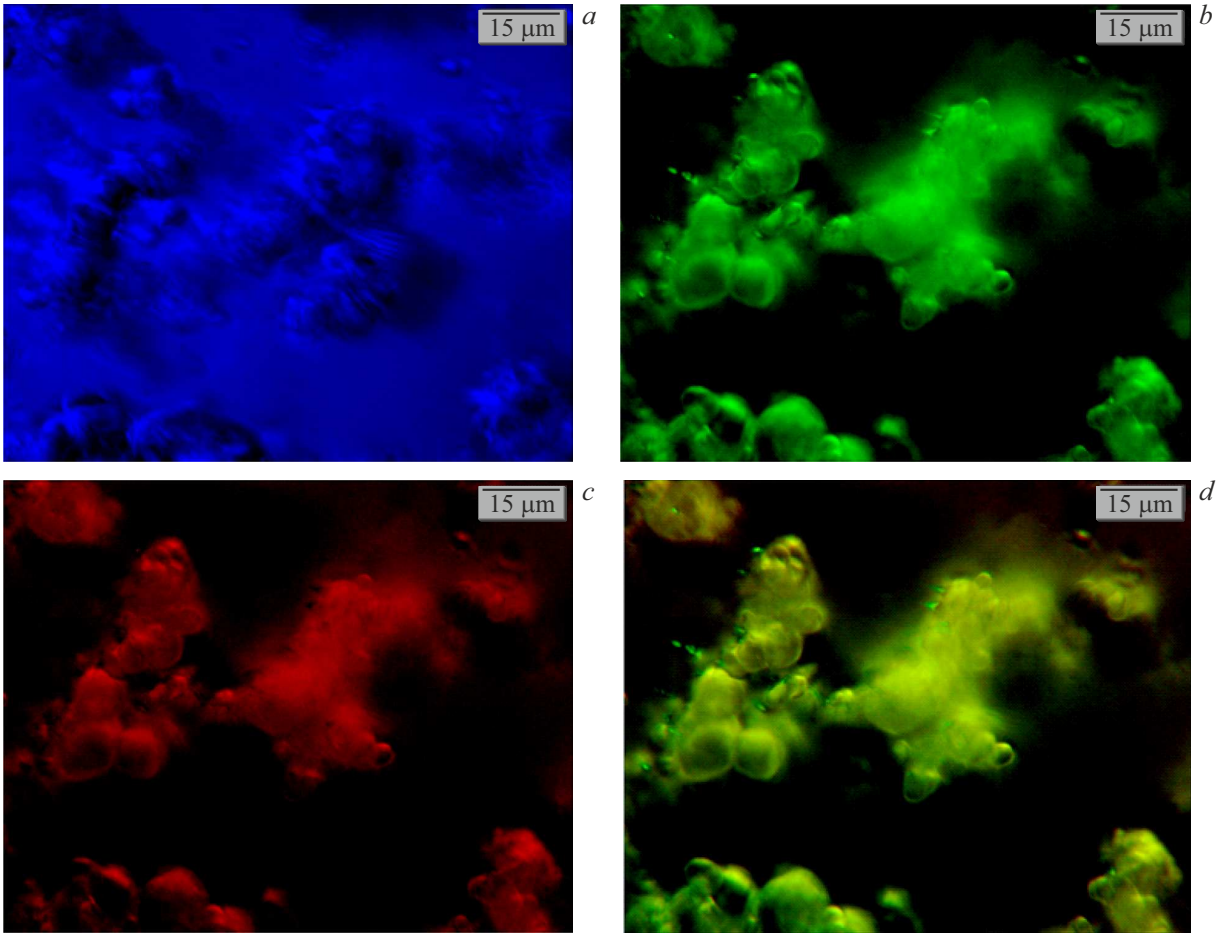

Figure 6. (*a*) The intensity distribution (in channel blue) of the FLS-540 phosphor was the least informative. The drop in intensity of the excitation light as a result of absorption and glare can be associated with phosphor crystals. (*b*) Intensity distribution (in channel green) of phosphor FLS-540 when illuminated simultaneously with white and blue LEDs. (*c*) Luminescence intensity distribution (in the red channel) of phosphor FLS-540 when illuminated simultaneously by white and blue LEDs. (*d*) Image of crystal luminescence cleaned from excitation radiation (result of combining the distributions in Figs. *c* and *b*).

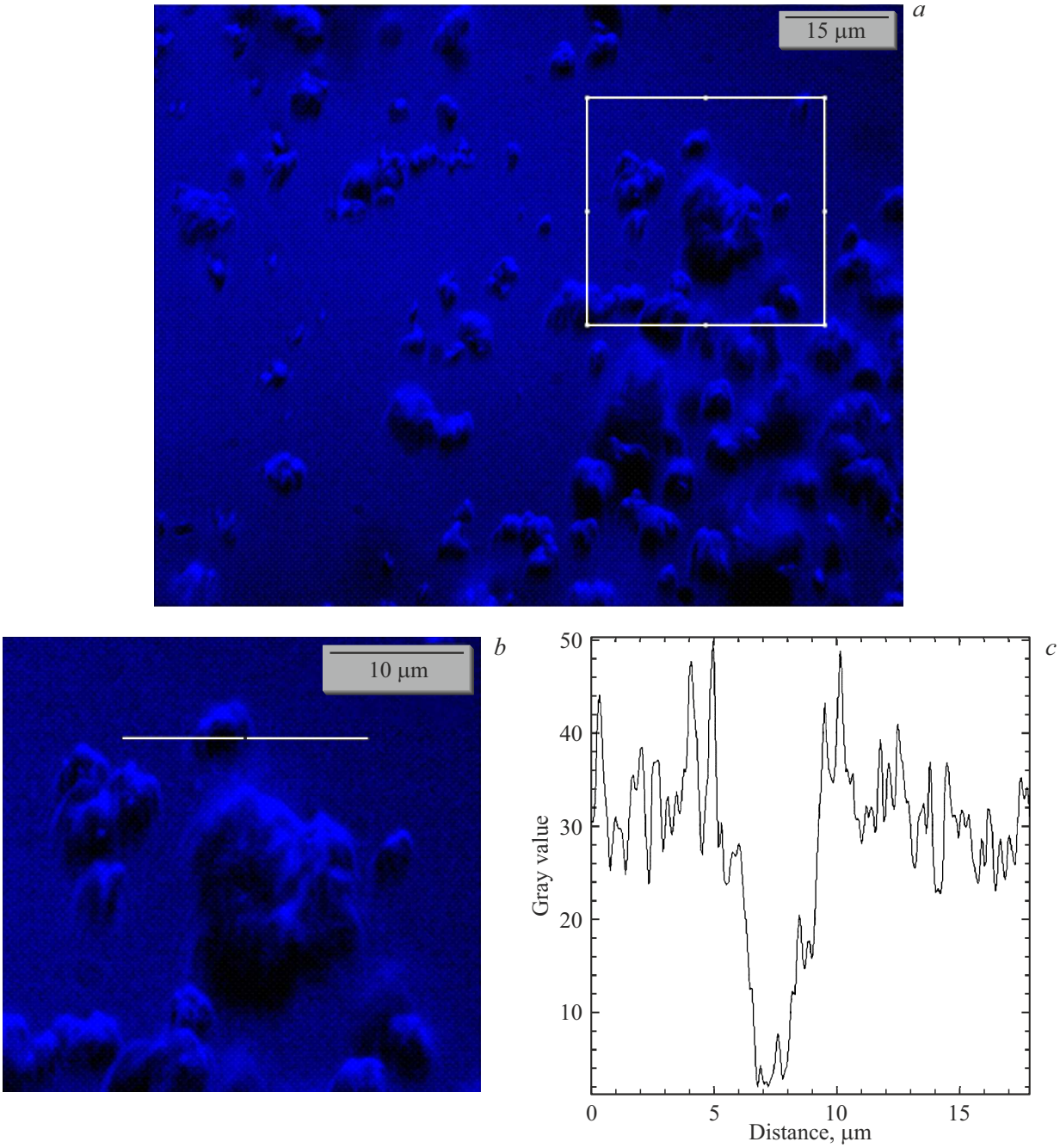

Figure 7. (*a*) Intensity distribution (in blue channel) of LSID-560 phosphor. No microcrystal luminescence was observed in the red and blue image channels.(*b*) The image of the selected area of the image in the Fig. *a*. (*c*) Profile of the light intensity distribution (in conditional units) along the diametric cross section of a microcrystal (shown by a line in the image). Light absorption of a microcrystal with a transverse size of about $4\,\mu$m visualized its boundaries in profile.

560, microcrystals with smaller size prevail (2−4 times) compared to the size of microcrystals of phosphor FLS-540. In addition, the surface of these crystals is much less smooth compared to FLS-540, as observed in Figs. 1 and 6. The analysis of the luminous flux shows that the luminous flux of the FLS-540 phosphor exceeds that of the LSID-560 phosphor under the same conditions of laser diode injection with $\lambda = 400-480$ nm, which indicates the influence of the size and shape (smoother and less smooth) of phosphor microcrystals on its photoluminescence parameters.

Thus, the present paper considers a method of determining the geometric and optical parameters of individual phosphor particles used for laser illumination devices using microscopy. Using the example of a fine-dispersed suspension of phosphors, phase images were obtained and optical

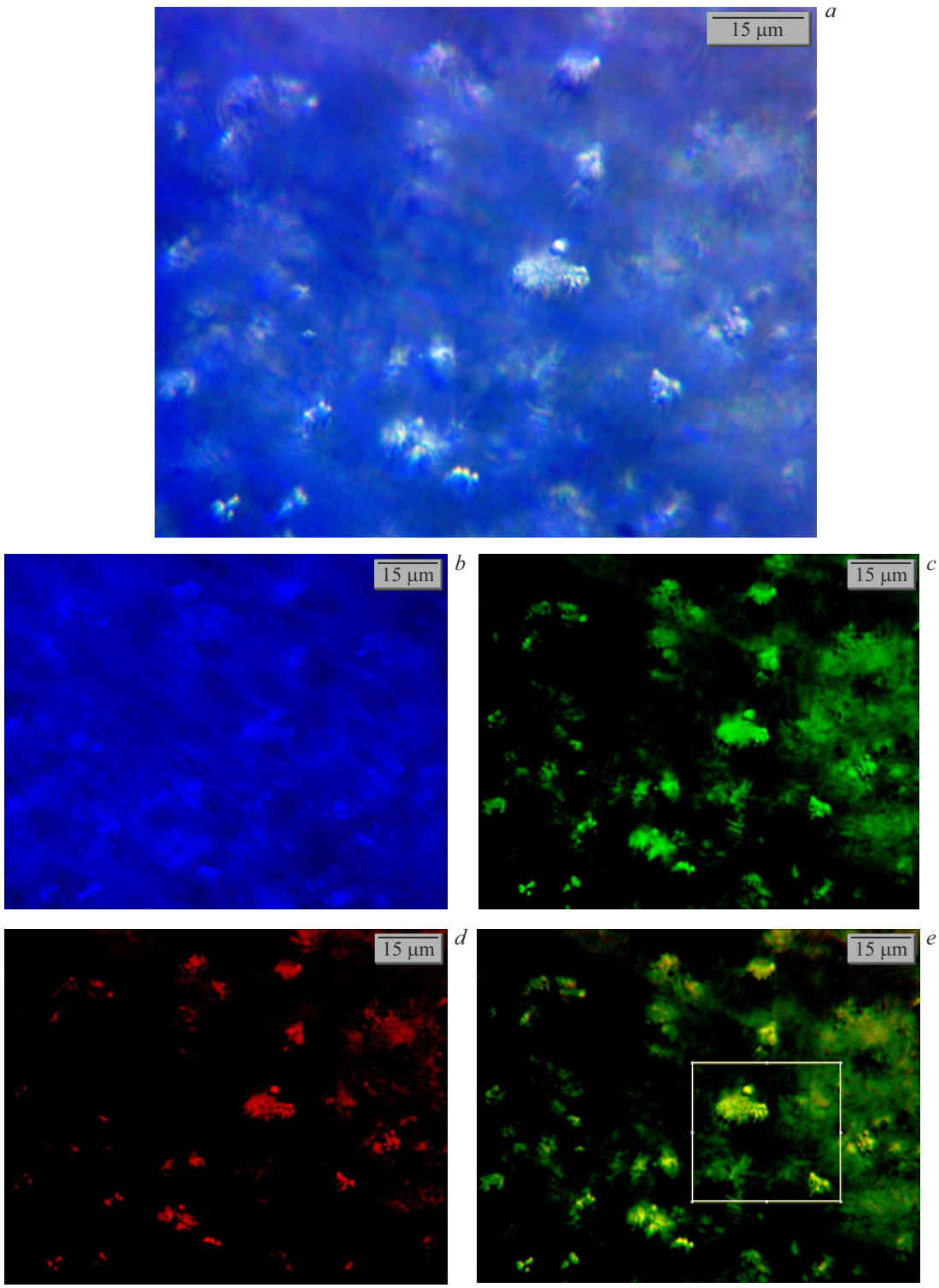

Figure 8. (*a*) With additional illumination of the LSID-560 phosphor with a white LED, an image was obtained in which a broadband conversion of the phosphor emission was observed. (*b*) The intensity distribution (in channel blue) of the LSID-560 phosphor is the least informative. The drop in intensity of the excitation light as a result of absorption and glare can be associated with phosphor crystals.(*c*) Intensity distribution (in channel green) of LSID-560 phosphor when illuminated simultaneously with white and blue LEDs. (*d*) Intensity distribution (in channel red) of LSID-560 phosphor when illuminated simultaneously by white and blue LEDs. (*e*) Image of crystal luminescence cleaned from excitation radiation (result of combining luminescence intensity distributions in Figs. *c* and *d*). (*f*) The image of the selected part of the image *e*. (*g*) Luminescence intensity distribution along the cross section of the microcrystal (shown by the line in the image on the left). The profile of luminescence intensity distribution shows microcrystal boundaries with a transverse size of $4\,\mu$m.

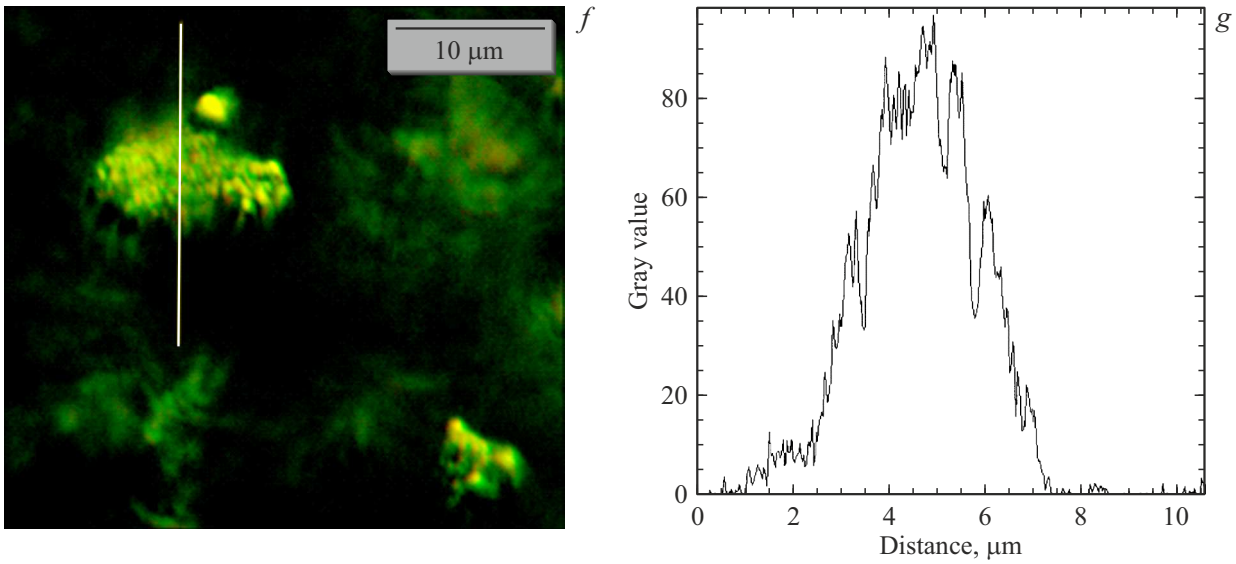

Fig. 8. Continuation.

parameters of individual particles with diameters from 40 to 150 nm were determined.

These studies demonstrate the high resolution of the microscopy method and can be used to visualize phosphor particles.

Funding

This study was supported by a grant from the Russian Science Foundation №23-29-00079, https://rscf.ru/project/23-29-00079/.

Conflict of interest

The authors declare that they have no conflict of interest.

References

[1] B. Bhaduri, H. Pham, M. Mir, G. Popescu. Optics Lett., **37** (6), 4 (2012). DOI: 10.1364/OL.37.001094
[2] S.M. Zuev, D.O. Varlamov, V.V. Kuksa. Pribory i tekhnika eksperimenta **6**, 57 (2022) (in Russian). DOI: 10.31857/S0032816221060148
[3] S.M. Zuev, D.O. Varlamov, V.V. Kuksa, V.P. Averin, S.V. Korniliev Sb. dokl. MNTK IPTIP RTU MIREA, **311** (2022). (in Russian).
[4] S.M. Zuev, D.O. Varlamov, D.A. Prokhorov. Voprosy electrotechnologii, **4**, 28 (2022). (in Russian).
[4] M. Fanous, M.P. Caputo, Y. Jae Lee, L.A. Rund, C. Best-Popescu, M.E. Kandel, R.W. Johnson, T. Das, M.J. Kuchan, G. Popescu. PLOS ONE, **15** (11), e0241084 (2020). DOI: 10.1371/journal.pone.0241084
[5] Z. Wang, L. Millet, M. Mir, H. Ding, S. Unarunotai, J. Rogers et al. Optics Express, **19** (2), 16 (2011). DOI: 10.1364/OE.19.001016
[6] C. Joo, T. Akkin, B. Cense, B.H. Park, J.F. de Boer. Opt. Lett., **30** (16), 2131 (2005). DOI: 10.1364/OL.30.002131
[7] Y. Zhao, G. Popescu. Optics Express, **30** (26), 47280 (2022). DOI: 10.1364/OE.474294
[8] N. Ozana, N. Lue, M. Renna, M.B. Robinson, A. Martin, A.I. Zavriyev, B. Carr, D. Mazumder, M.H. Blackwell, M.A. Franceschini, S.A. Carp. Front. Neurosci, **16**, 1 (2022). DOI: 10.3389/fnins.2022.932119
[9] X. Cheng, D. Tamborini, S.A. Carp, O. Shatrovoy, B. Zimmerman, D. Tyulmankov et al. Opt. Lett., **43**, 2756 (2018). DOI: 10.1364/OL.43.002756
[10] L. Colombo, M. Pagliazzi, S.K.V. Sekar, D. Contini, A.D. Mora, L. Spinelli et al. Neurophotonics, **6** (3), 035001(2019). DOI: 10.1117/1.NPh.6.3.035001

Translated by Y.Deineka